Flight control system design of UAV with wing incidence angle simultaneously and stochastically varied

Metin Uzun
Department of Aircraft Maintenance and Repair, Iskenderun Technical University, Iskenderun, Turkey

Abstract

Purpose – This study aims to simultaneously and stochastically maximize autonomous flight performance of a variable wing incidence angle having an unmanned aerial vehicle (UAV) and its flight control system (FCS) design.

Design/methodology/approach – A small UAV is produced in Iskenderun Technical University Drone Laboratory. Its wing incidence angle is able to change before UAV flight. FCS parameters and wing incidence angle are simultaneously and stochastically designed to maximize autonomous flight performance using an optimization method named simultaneous perturbation stochastic approximation. Obtained results are also benefitted during UAV flight simulations.

Findings – Applying simultaneous and stochastic design approach for a UAV having passively morphing wing incidence angle and its flight control system, autonomous flight performance is maximized.

Research limitations/implications – Permission of the Directorate General of Civil Aviation in Turkish Republic is necessary for real-time flights.

Practical implications – Simultaneous stochastic variable wing incidence angle having UAV and its flight control system design approach is so useful for maximizing UAV autonomous flight performance.

Social implications – Simultaneous stochastic variable wing incidence angle having UAV and its flight control system design methodology succeeds confidence, excellent autonomous performance index and practical service interests of UAV users.

Originality/value – Creating an innovative method to recover autonomous flight performance of a UAV and generating an innovative procedure carrying out simultaneous stochastic variable wing incidence angle having UAV and its flight control system design idea.

Keywords UAVs, Wing incidence Angle, Flight control system, PID controller, Simultaneous stochastic design, Autonomous flight performance

Paper type Research paper

1. Introduction

Over the past quarter century, unmanned air vehicles (UAVs) have been widely used not only for military missions but also for commercial missions because of the fact that these unmanned vehicles have many benefits with respect to the traditional manned vehicles. Being cheap during production and tasks, easy variation for configuration with respect to the customer requests and not endangering the pilot's life on difficult missions are the main advantages of these vehicles. UAVs have been commonly applied for civilian missions such as agriculture and aerial photography. They have been also applied in military missions such as in the army for surveillance of enemy activity and in Air Force for radar system jamming (please see Austin, 2010) for many other UAV missions).

For the traditional UAV design methodology, a dynamic model of any physical system to be controlled is served *a priori* to the control engineer who has no influence on the design of this system. However, there is a well-known reality that the dynamic model design is not irrelevant with control model design (please see Grigoriadis *et al.*, 1993; Grigoriadis *et al.*, 1996; Oktay and Sultan, 2013, for details of this reality). Small variations over some of the dynamic model parameters may improve autonomous performance remarkably. The traditional design methodology does not denote the optimum complete design. In sophisticated methodology, the dynamic model to be controlled and the control model is necessary to be simultaneously designed while minimizing a cost function. In this research article, this reality is considered and a small UAV (i.e. Iskenderun Technical University [ISTE]-UAV), which is manufactured in Iskenderun Technical University, and an autonomous system are simultaneously designed over wing incidence angle parameter and autonomous system parameters while minimizing a cost function capturing some flight trajectory tracking parameters (i.e. settling time, rise time and maximum overshoot for both longitudinal and lateral flights).

Some studies in the literature have been applied to variation of wing incidence angle for examining the effects of it on some different aircraft performance criteria. For example, in Sedin

The current issue and full text archive of this journal is available on Emerald Insight at: **https://www.emerald.com/insight/1748-8842.htm**

Aircraft Engineering and Aerospace Technology
96/5 (2024) 715–725
 [ISSN 1748-8842]
[DOI 10.1108/AEAT-11-2023-0287]

Received 8 November 2023
Revised 2 January 2024
10 February 2024
28 March 2024
17 April 2024
Accepted 14 May 2024

et al. (2004), computational analysis and re-design of a wing-strake combination was followed. Computational analysis and re-design of a baseline wing-strake configuration using 3D Navier–Stokes calculations was done. In this study, it was obtained that improvements were found in low-speed high-lift conditions with minor differences in also wing incidence angle in high-speed transonic. In Boling and Zha (2021), the longitudinal static stability of a tandem-wing CoFlow Jet VTOL (CFJ-VTOL) aircraft concept with high-speed cruise Mach number of 0.6 was numerically researched. It was found that increasing the loading on the front wing by increasing its incidence angle enhances the pitching moment coefficient. Eventually, it was also reached that the pitching moment should be positive at lower angles of attack when the lift coefficient is zero. A similar conclusion is obtained by reducing the incidence angle of the rear wing. In Harvey *et al.* (2022), it was declared that aircraft wing incidence angle has important effect on longitudinal pitch stability, control and maneuverability. In Raymer (1992), it was also mentioned that wing incidence angle can be selected to minimize drag during some operating conditions, generally cruise. This angle is required to be selected such that the wing has the correct angle of attack for the chosen design situation, the fuselage has the angle of attack for minimum drag [please also see Gaspari and Moens (2019); Moens (2019); Silva *et al.* (2023) for different applications of wing incidence angle for enhancing some different performance criteria and see Oktay *et al.* (2016); Coban (2020); Sahin *et al.* (2022); Sal (2023); Kose and Oktay (2023) for different simultaneous aerospace design applications].

In this article at the beginning, effect of wing incidence angle on UAV dynamic models is presented. After that, brief introduction for the manufactured UAV called as ISTE-UAV is given. Then, reference autonomous system is shortly explained. The optimization algorithm applied for simultaneous design of UAV and autonomous system is also explained. In the end, the results of simultaneous design methodology are mentioned in detail. This article in the literature is the *first article* simultaneously and stochastically designing an UAV having varying wing incidence angle and its autonomous system. In addition, by following this methodology a stochastic optimization technique that is simultaneous perturbation stochastic approximation (SPSA) is also *first time* applied in the relevant literature. This fulfills obtaining the optimal results safe and fast.

2. Effect of wing incidence angle on unmanned aerial vehicle dynamic models

Here effect of varying wing incidence angle on UAV dynamic models is given. In Figure 1, photo of our varying wing incidence angle having UAV named as ISTE-UAV is shared (see appendix for some specific physical data of our UAV). This UAV platform is chosen because it has been applied in many UAV research studies (e.g. Coban, 2020; Uzun and Oktay, 2023) by ISTE before.

In this research article, flight simulations are applied by benefitting linearized models of this UAV platform. The generic longitudinal and lateral state space models of any fixed-wing UAV are presented in equation 1(a) and 1(b), respectively

Figure 1 Photo of ISTE-UAV having varying wing incidence angle

Source: Figure courtesy of Uzun

[visit Etkin and Reyd (1996), Chapter IV p. 112 and 113; Nelson (2007), Chapter IV equation 4.51 and Chapter V equation 5.33 for much more details and also visit nomenclature in the Appendix for relevant symbols]:

$$\begin{bmatrix} \Delta\dot{u} \\ \Delta\dot{w} \\ \Delta\dot{q} \\ \Delta\dot{\theta} \end{bmatrix} = \begin{bmatrix} X_u & X_w & 0 & -g \\ Z_u & Z_w & u_0 & 0 \\ M_u + M_{\dot{w}} Z_w & M_w + M_{\dot{w}} Z_w & M_q + M_{\dot{w}} u_0 & 0 \\ 0 & 0 & 1 & 0 \end{bmatrix} \times \begin{bmatrix} \Delta u \\ \Delta w \\ \Delta q \\ \Delta\theta \end{bmatrix} + \begin{bmatrix} X_{\delta_T} & X_{\delta_e} \\ Z_{\delta_T} & Z_{\delta_e} \\ M_{\delta_T} + M_{\dot{w}} Z_{\delta_T} & M_{\delta_e} + M_{\dot{w}} Z_{\delta_e} \\ 0 & 0 \end{bmatrix} \begin{bmatrix} \Delta\delta_T \\ \Delta\delta_e \end{bmatrix} \quad (1a)$$

$$\begin{bmatrix} \Delta\dot{v} \\ \Delta\dot{p} \\ \Delta\dot{r} \\ \Delta\dot{\phi} \end{bmatrix} = \begin{bmatrix} Y_v & Y_p & -(u_0 - Y_r) & -g\cos(\theta_0) \\ L_w^* + \frac{I_{xz}}{I_x} N_v^* & L_p^* + \frac{I_{xz}}{I_x} N_p^* & L_r^* + \frac{I_{xz}}{I_x} N_r^* & 0 \\ N_v^* + \frac{I_{xz}}{I_z} L_v^* & N_p^* + \frac{I_{xz}}{I_z} L_p^* & N_r^* + \frac{I_{xz}}{I_z} L_r^* & 0 \\ 0 & 1 & 0 & 0 \end{bmatrix} \times \begin{bmatrix} \Delta v \\ \Delta p \\ \Delta r \\ \Delta\phi \end{bmatrix} + \begin{bmatrix} 0 & Y_{\delta_r} \\ L_{\delta_a}^* + \frac{I_{xz}}{I_x} N_{\delta_a}^* & L_{\delta_r}^* + \frac{I_{xz}}{I_x} N_{\delta_r}^* \\ N_{\delta_a}^* + \frac{I_{xz}}{I_z} L_{\delta_a}^* & N_{\delta_r}^* + \frac{I_{xz}}{I_z} L_{\delta_r}^* \\ 0 & 0 \end{bmatrix} \begin{bmatrix} \Delta\delta_a \\ \Delta\delta_r \end{bmatrix} \quad (1b)$$

In equations 1(a) and 2(b), most of the stability derivatives change with respect to the wing incidence angle. For instance, some of the stability derivatives: X_u, Z_u, Y_p change with respect to the wing incidence angle as following (visit Appendix for also descriptions of all of the symbols in equations (1) and (2):

Figure 2 Sketch of any UAV having varying wing incidence angleNote: I_w is the original wing incidence angle, and I_w_last is the stochastically optimized wing incidence angle.

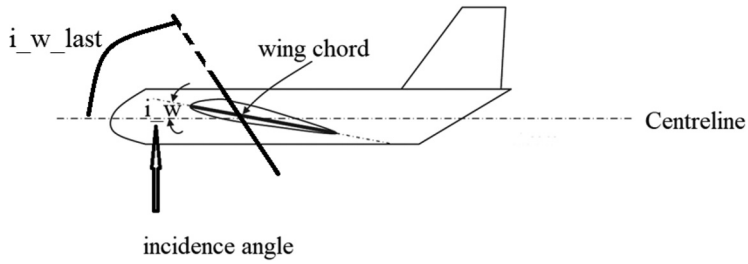

Note: I_w is the original wing incidence angle, and I_w_last is the stochastically optimized wing incidence angle
Source: Figure courtesy of Uzun

Figure 3 Block diagram of the hierarchical autonomous system

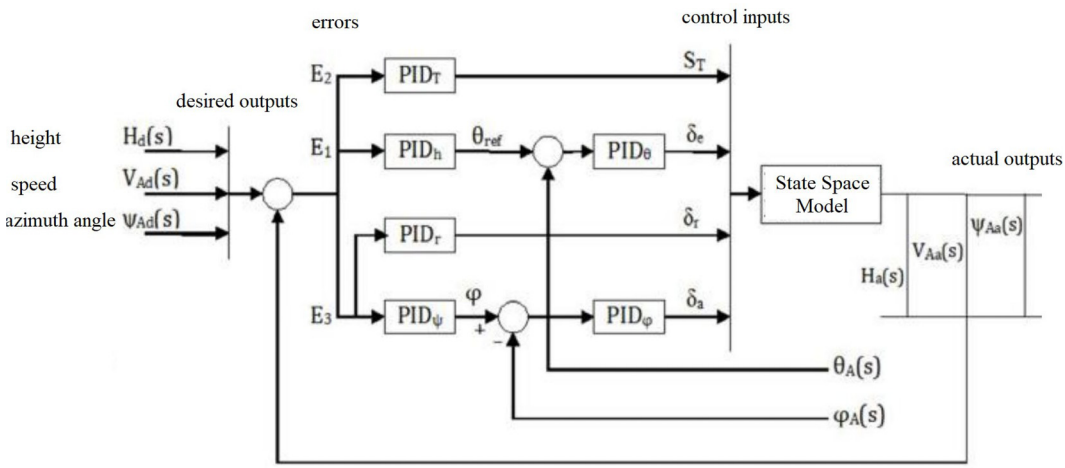

Source: Figure courtesy of Uzun

Figure 4 Block diagram of simultaneous stochastic design

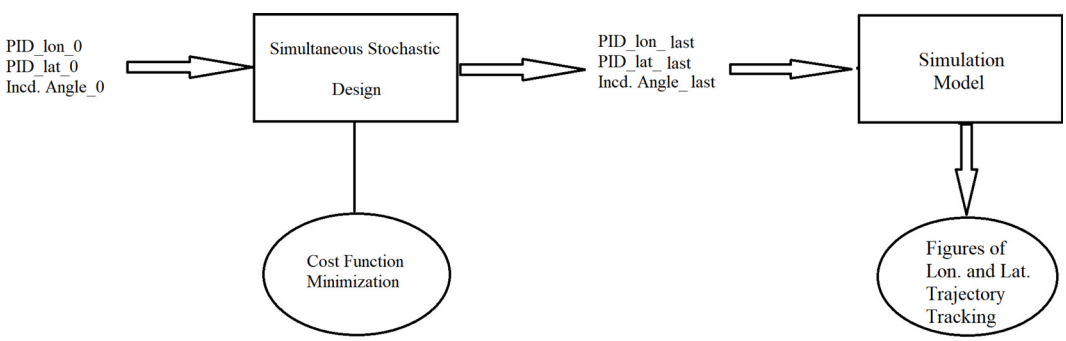

Source: Figure courtesy of Uzun

Aircraft Engineering and Aerospace Technology
Volume 96 · Number 5 · 2024 · 715–725

$$X_u = \frac{-(C_{D_u} + 2C_{D_0})QS}{mu_0} \quad \text{where} \quad C_{X_u} = -(C_{D_u} + 2C_{D_0}) + C_{T_u} \tag{2a}$$

$$Z_u = \frac{-(C_{L_u} + 2C_{L_0})QS}{mu_0} \quad \text{where} \quad C_{Z_u} = -\frac{M^2}{1 - M^2} c_{L_0} \tag{2b}$$

$$Y_p = \frac{QSb}{m} c_{M_p} \quad \text{where} \quad C_{Y_p} = c_L \frac{AR + \cos\Lambda}{AR + 4\cos\Lambda} \tan\Lambda \tag{2c}$$

Above C_{D_0}, C_{L_0} and C_L are affected by wing incidence angle considerably. For variation of other stability parameters with respect to the wing incidence angle please refer to Etkin (1997) Chapter IV and Nelson (2007) Chapter IV and V can be seen. During simultaneous stochastic design methodology, the linearized model mentioned above and autonomous system are redesigned for maximizing autonomous flight performance index capturing parameters relevant with trajectory tracking of longitudinal and lateral motions (Figure 2).

Figure 5 Stochastic optimization results

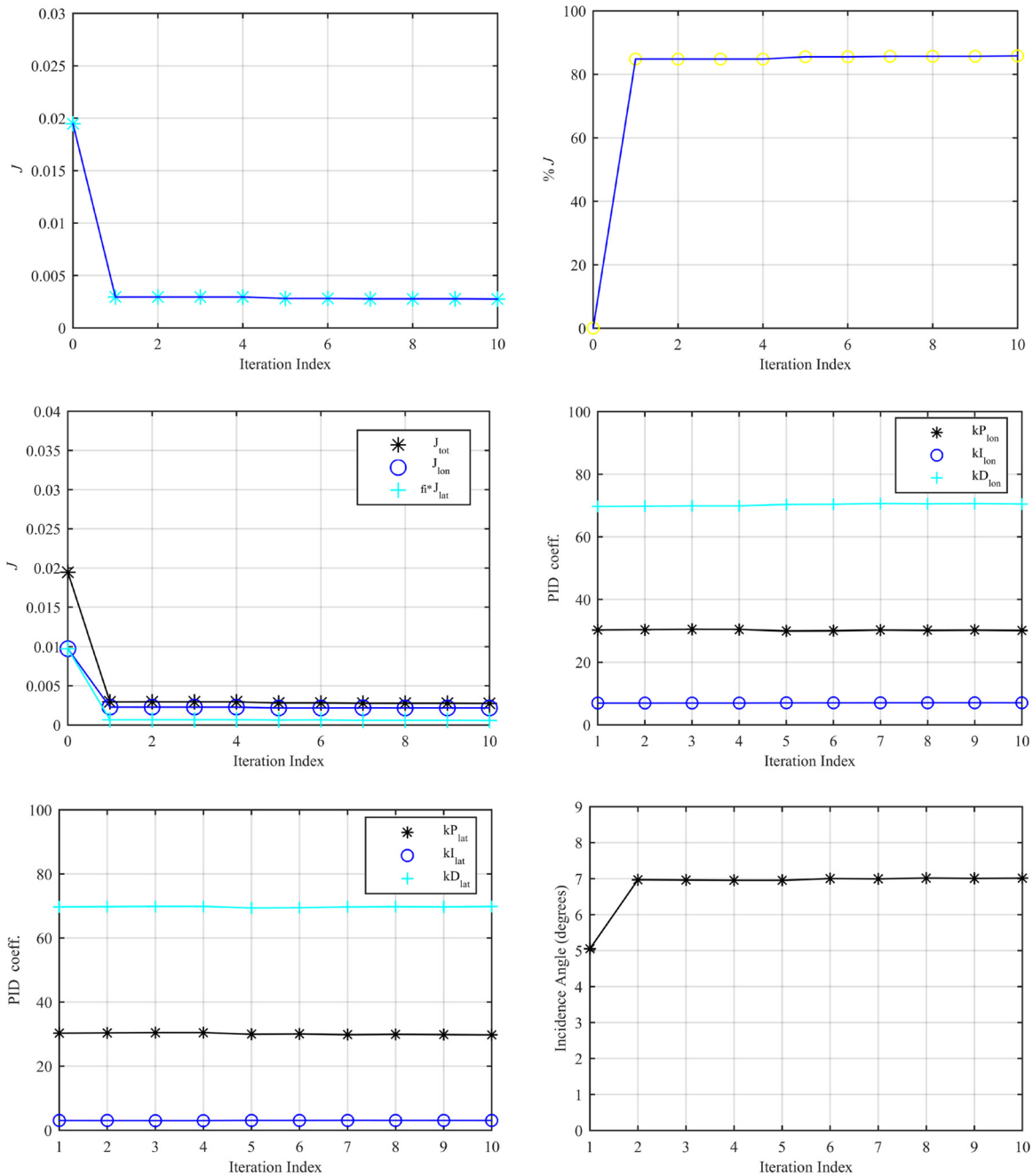

Source: Figure courtesy of Uzun

3. Reference autonomous system

Here, a hierarchical autonomous system capturing PID-based layers inside is selected for trajectory tracking of varying wing incidence angle having ISTE-UAV. Its main properties are presented next: Any hierarchical autonomous system applied for UAV autonomy has three layers inside that are outer, middle and inner layers. Behaviors of roll and pitch angles are stabilized in most inside layer through benefitting control signals that are elevator variation angle and aileron variation angle. Then, heading and altitude behaviors are stabilized in the middle layer. Finally, tracking of x- and y-positions of UAV is put into practice in the outer layer. This type of autonomous system has six PID controllers inside of the autonomous block diagram. By applying this block diagram, three relevant reference inputs that are altitude, speed and heading angle can be pursued in the most general sense (see also Oktay *et al.*, 2016; Coban, 2020; Sahin *et al.*, 2022; Kose and Oktay, 2023, for more details). In Figure 3, block diagram of the traditional hierarchical autonomous system is given.

4. Reference optimization algorithm for simultaneous stochastic design

The simultaneous stochastic varying wing incidence angle having UAV and its FCS design problem for minimizing cost function is presented in this section. Here, the cost function is evaluated by $\mathcal{J} = \mathcal{J}_{lon} + \Phi * \mathcal{J}_{lat}$ (i.e. capturing terms related with both longitudinal and weighted lateral trajectory tracking), and there exist also lower and upper bounds on these relevant design parameters (i.e. $k_{P_{lon}}, k_{I_{lon}}, k_{D_{lon}}, k_{P_{lat}}, k_{I_{lat}}, k_{D_{lat}}, \Theta_{w_i}$ where these parameters are longitudinal and lateral PID controller gains and incidence angle of wing, respectively and Φ is the coefficient obtained by dividing the initial longitudinal cost to initial lateral cost). In this study, longitudinal flight means tracking of UAV pitch angle and lateral flight means tracking of roll angle. Here, longitudinal and lateral flights are considered simultaneously. There is a problem for design that evaluation of cost function derivatives with respect to these design parameters is analytically impossible. Owing to the this fact, definite stochastic optimization methods are needed. For solving this specific design problem, a definite stochastic optimization methodology called as SPSA is selected here. Stochastic optimization technique SPSA has many superiorities with respect to the current methodologies in the relevant literature. First, SPSA is inexpensive since it only uses two evaluations of the objective for guessing the gradient. As a consequence, it is more efficient in finding the global minimum than other computationally expensive algorithms such as genetic algorithms and simulated annealing and also much faster than other known stochastic optimization methodologies such as genetic algorithms and simulated annealing (see Sadegh and Spall, 1998; He *et al.*, 2003). Additionally, it is likewise useful for solving constrained optimization problems (see Oktay *et al.*, 2016; Coban, 2020; Sahin *et al.*, 2022; Sal, 2023; Kose and Oktay, 2023, for similar applications). It also fulfills fast convergence of relevant algorithm as well as safe optimum outcomes fast. Here, SPSA is chosen for the first time in the literature for simultaneous stochastic UAV having varying wing incidence angle and its FCS design methodology.

A short explanation of SPSA algorithm is presented next: Ψ symbolizes the vector of optimization parameters (i.e. $k_{P_{lon}}, k_{I_{lon}}, k_{D_{lon}}, k_{P_{lat}}, k_{I_{lat}}, k_{D_{lat}}, \Theta_{w_i}$ in this research article which are six gains of PID-based hierarchical autonomous system for longitudinal and lateral motions as well as one incidence angle of wing). For the classical SPSA, if $\Psi_{[k]}$ is the prediction of Ψ at k-th iteration, then $\Psi_{[k+1]} = \Psi_{[k]} - \Psi_k\, g_{[k]}$, where $g_{[k]}$ is the guess of the objective's gradient at $\Psi_{[k]}$ and evaluated by $g_{[k]} = \left[\frac{\Gamma_+ - \Gamma_-}{2d_k\Delta_{[k]1}} \ldots\ldots \frac{\Gamma_+ - \Gamma_-}{2d_k\Delta_{[k]p}}\right]^T$, $a_{[k]}$ and d_k are gain sequences, $\Delta_{[k]} \in R^p$ is a vector of p mutually independent mean-zero random variables $\{\Delta_{[k]}1 \ldots \Delta_{[k]}p\}$ fulfilling definite circumstances), Γ_+ and Γ_- are predictions of the objective calculated at $\Psi_{[k]} + d_{[k]}\Delta_{[k]}$ and $\Psi_{[k]} - d_{[k]}\Delta_{[k]}$ (visit Sadegh and Spall, 1998; He *et al.*, 2003). An algorithm of SPSA for application of simultaneous stochastic design of UAV is given below:

- Step 1: Set $k = 1$ and select initial values for the optimization variables, $\Psi = \Psi_{[k]}$, and a particular flight situation.
- Step 2: Calculate A_p and B_p using $\Psi = \Psi_{[k]}$, design the corresponding PID controllers and obtain the current value of the objective, Γ_k.
- Step 3: Perturb $\Psi_{[k]}$ to $\Psi_{[k]} + d_{[k]}\Delta_{[k]}$ and $\Psi_{[k]} - d_{[k]}\Delta_{[k]}$ and solve the equivalent PID design problems to get Γ_+ and Γ_-, respectively. Then calculate the approximate gradient, $g_{[k]}$ with $d_{[k]}$.
- Step 4: If $\|a_k g_{[k]} < \delta\psi\|$, and $\delta\Psi$ is the minimum permitted variation of Ψ or $k+1$ is greater than the maximum number of iterations allowed, exit, else calculate the next guess of Ψ, $\Psi_{[k+1]}$, using $\Psi_{[k+1]} = \Psi_{[k]} - a_{[k]}g_{[k]}$, set $k = k+1$ and return to Step 2.

5. Results of simultaneous stochastic design methodology

In this research article simultaneous stochastic varying wing incidence angle having UAV and it flight control system design methodology is evaluated. In this example for longitudinal autonomous system, it is necessary to follow five degrees of aircraft pitch angle, and for lateral autonomous system, it is necessary to follow five degrees of aircraft roll angle concurrently. The autonomous performance cost function in

Table 1 Summary of initial and final optimum results

Parameter	Initial Value	Optimum value
Incidence angle (degree)	5	7.03
P_lon	50	29.79
I_lon	5	7.04
D_lon	50	70.84
P_lat	50	29.43
I_lat	5	3.02
D_lat	50	70.15
Cost_lon	9.73 e-3	2.10 e-3
Cost_lat	20.4 e-3	20.3 e-4
Cost_tot	19.46 e-3	3.06 e-3

Note: $J = J_{lon} + \Phi * J_{lat}$ where $\Phi = (9.73 / 20.4)$ in this study
Source: Table courtesy of Uzun

this research article capturing terms relevant with not only for longitudinal flight but also for lateral flight (i.e. consisting of rise time, settling time and overshoot during relevant path tracking). Simultaneous stochastic design of dynamical system and autonomous flight control system is put into practice here. After applying simultaneous stochastic design methodology rather than applying traditional sequential methodology, much more cost function save is found (please see relevant block diagram in Figure 4 for summary of related approach). In the traditional sequential methodology first of all dynamical system is modeled and after that autonomous flight control system is designed whereas in our novel methodology dynamical system and autonomous flight control system are simultaneously and stochastically redesigned for reaching the best performance. Here the best performance means minimizing a cost function capturing terms related with both longitudinal and lateral reference trajectory tracking. Rise time, settling time and overshoot are benefited for determining quality of reference trajectory tracking. In Figure 5, total performance cost improvement (5a), relative total performance cost improvement (5b), longitudinal

Figure 6 Longitudinal closed-loop responses of ISTE-UAV

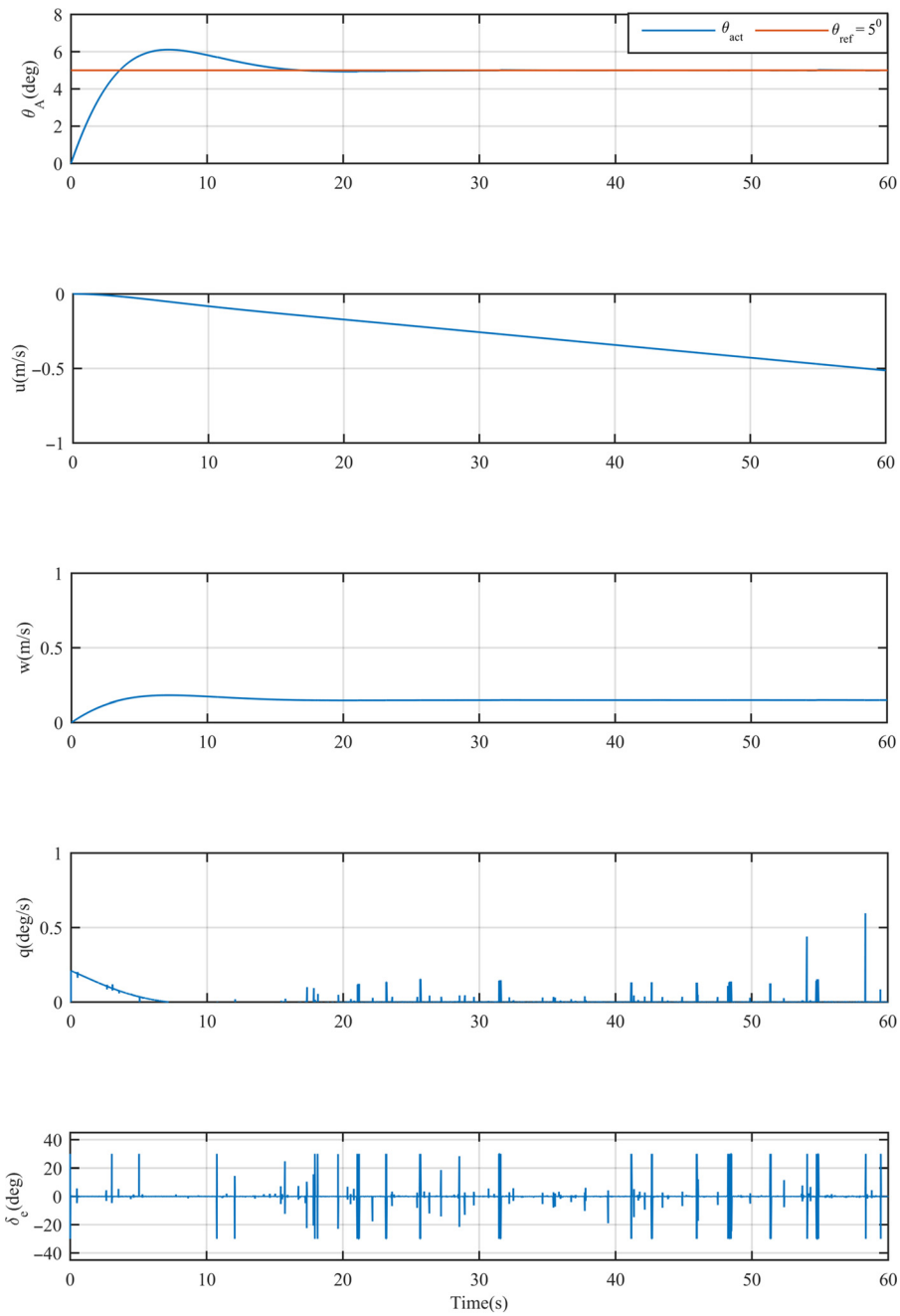

Source: Figure courtesy of Uzun

performance cost improvement (5c), weighted lateral performance cost improvement (5c), total performance cost improvement (5c), changes of longitudinal PID controller gain parameters (5d), changes of lateral PID controller gain parameters (5e) and, finally, change of wing incidence angle (5f) are presented. The relative total performance cost function save with respect to the default preliminary situation (i.e. $p = 50$, I = 5, D = 50 for both longitudinal and lateral PID controllers, initial 5 degree of wing incidence angle) is almost %86 after using simultaneous stochastic design methodology. In addition, in Figure 4 for the first step of iteration, the number "0" is selected and it corresponds to the default values. Furthermore, the resulted values of design parameters are $p = 29.79$, I = 7.04, D = 70.84 for longitudinal PID controller, and $p = 29.43$, I = 3.02, D = 70.15 for lateral PID controller, and 7.02 degree of wing incidence angle (please see the Table 1 for values of initial and optimum situations).

Achievement of hierarchical autonomous flight control system during existence of the minor turbulence on the dynamical system is evaluated as well by applying MATLAB and Simulink in simulation environment. The longitudinal motion closed-loop system responses during existence of pure turbulence on the dynamical system are given in Figure 6. It is required to be noted that in Figures 6 and 7, the x-axis symbolizes time in seconds and y-axis symbolizes output of interest with degrees. For the other symbols existing in the figures nomenclature existing at Appendix can be examined. It can be openly seen from Figure 6 that during existence of turbulence on the dynamical system, the hierarchical autonomous flight control system is able to successfully follow the reference longitudinal trajectory. The settling time, rise time and overshoot values are unimportant because of the application of the simultaneous stochastic design methodology formerly mentioned. Additionally, other states, for instance longitudinal and vertical velocity states (i.e. u and w), which are not in major interest for longitudinal motion trajectory tracking do not face to face fast and large oscillations during tracking of

Figure 7 Lateral closed-loop responses of ISTE-UAV

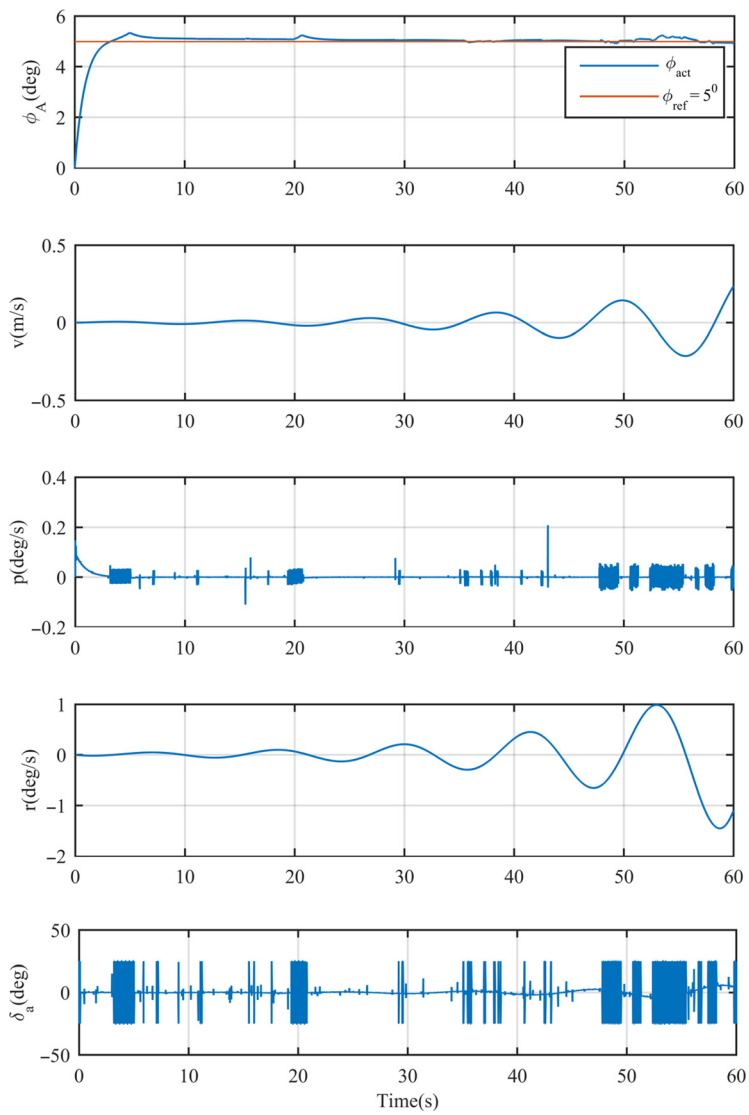

Source: Figure courtesy of Uzun

Figure 8 Comparison of initial and final closed-loop responses of ISTE-UAV

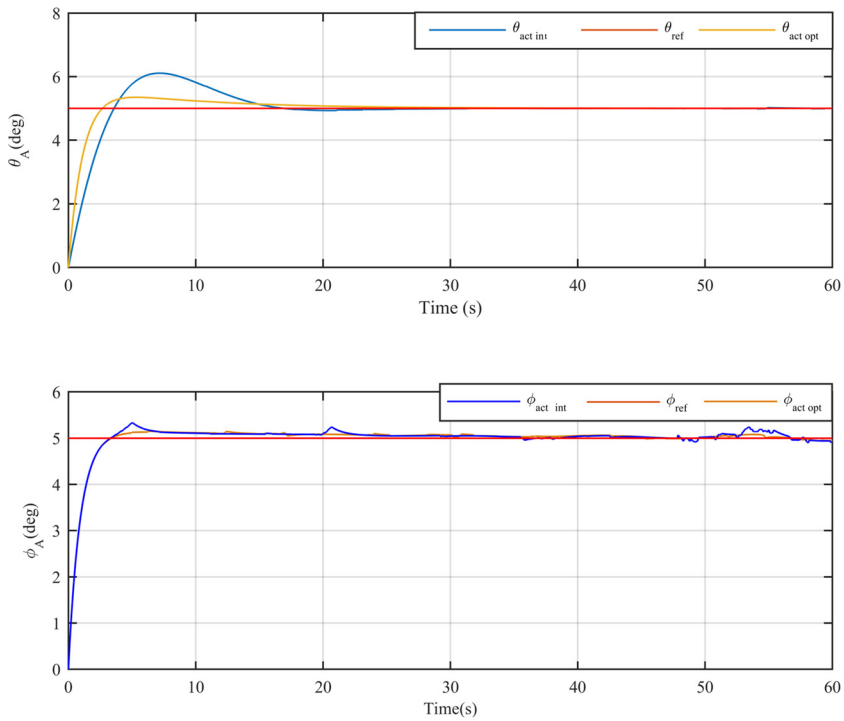

Source: Figure courtesy of Uzun

longitudinal motion trajectory. Finally, during the existence of bound on control surface (±30 degrees for elevator in this research particle), desired longitudinal motion trajectory is followed effectively.

Achievement of hierarchical autonomous flight control system during existence of minor turbulence on the lateral dynamical system is also considered. In Figure 7, the lateral closed-loop system responses during existence of pure turbulence on the lateral dynamical system are presented. It can be clearly determined from Figure 7 that during existence of pure turbulence on the dynamical system, the hierarchical autonomous flight control system can successfully follow the reference lateral motion trajectory that is the five degrees of roll angle of the UAV. The values of settling time, rise time and overshoot for lateral motion trajectory tracking are insignificant because of the use of simultaneous stochastic design methodology earlier mentioned. In addition, other states such as v and q that are not in principal interest for lateral motion trajectory tracking do not face to face fast and large oscillations during tracking of lateral motion trajectory. Finally, during the existence of bound on control surface (±25 degrees for aileron here), the desired lateral motion trajectory is followed successfully.

In Figure 8, the longitudinal and lateral closed-loop system trajectory tracking responses during the existence of pure turbulence on the dynamical systems are presented. Two scenarios are evaluated at the same time in Figure 8. These are initial situations before starting SPSA where $p = 50$, I = 5 and D = 50 for both PID controllers and wing incidence angle is equal to 5° and final situation after application of SPSA where optimum results can be found in Table 1. As there is %86 improvement in cost, the rise time, settling time and overshoot for the final situation is considerably smaller than the ones for the initial situation.

6. Conclusions

Simultaneous stochastic design of UAV having varying wing incidence angle and its flight control system design methodology is investigated for maximizing the autonomous flight performance of a particular UAV named ISTE-UAV. An UAV is produced in our ISTE-UAV Laboratory. Wing incidence angle of this UAV can vary passively before starting flight. Autonomous flight control system variables (i.e. parameters of longitudinal and lateral PID controllers) and wing incidence angle are simultaneously and stochastically redesigned for optimizing autonomous flight performance cost function by applying a stochastic optimization method named as SPSA. Obtained results are applied not only for longitudinal flight simulation but also for lateral flight simulation. Important improvement in autonomous flight performance is almost %86 with respect to the classical UAV, which does not have varying wing incidence angle, is found after use of simultaneous stochastic design methodology. This caused much less overshoot, much less settling time and much less rise time during tracking of relevant trajectories. In addition, relevant closed-loop responses during existence of the pure turbulence during flight is also investigated and reasonable results which mean that small rise time and small settling time and also small overshoot are obtained. This research article represents UAV users much more confident, high autonomous performing and peaceful utility having UAV possibility. In the future, it is planned to combine

many different passive and active morphing approaches applied in UAVs produced in ISTE-UAV Laboratory. It is also aimed to validate obtained simulations results with data logs of the real-time UAV flights in the close future.

References

Austin, R. (2010), *Unmanned Aircraft Systems*, Wiley, NJ.

Boling, J. and Zha, G.-C. (2021), "Numerical investigation of longitudinal static stability of a high-speed tandem-wing VTOL vehicle using CoFlow jet airfoil", AIAA SciTech Forum, 19-21 Jan 2021.

Coban, S. (2020), "Autonomous performance maximization of research-based hybrid unmanned aerial vehicle", *Aircraft Engineering and Aerospace Technology*, Vol. 92 No. 4, pp. 645-651.

Etkin, B. (1997), *Dynamics of Flight: Stability and Control*, 3rd ed.

Etkin, B. and Reyd, L.D. (1996), *Dynamics of Flight: Stability and Control*, John Wiley & Sons, New York, NY.

Gaspari, H.D. and Moens, F. (2019), "Aerodynamic shape design and validation of an advanced High-Lift device for a regional aircraft with morphing droop nose", *International Journal of Aerospace Engineering*, Vol. 2019, doi: 10.1155/2019/7982168.

Grigoriadis, K.M., Zhu, G. and Skelton, R.E. (1996), "Optimal redesign of linear systems", *Journal of Dynamic Systems, Measurement, and Control*, Vol. 118 No. 3, pp. 598-605.

Grigoriadis, K.M., Carpenter, M.J., Zhu, G. and Skelton, R.E. (1993), "Optimal redesign of linear systems", Proceedings of the American Control Conference, San Francisco, CA.

Harvey, C., Gamble, L.L., Bolander, R.C., Hunsaker, D.F., Joo, J.J. and Inman, D.J. (2022), "A review of avian-inspired morphing for UAV flight control", *Progress in Aerospace Sciences*, Vol. 132, pp. 1-27.

He, Y., Fu, M.C. and Marcus, S.I. (2003), "Convergence of simultaneous perturbation stochastic approximation for non-differentiable optimization", *IEEE Transactions on Aerospace and Electronic Systems*, Vol. 48 No. 8, pp. 1459-1463.

Kose, O. and Oktay, O. (2023), "Simultaneous design of morphing hexarotor and autopilot system by using deep neural network and SPSA", *Aircraft Engineering and Aerospace Technology*, Vol. 95 No. 6, pp. 939-949.

Moens, F. (2019), "Augmented aircraft performance with the use of morphing technology for a turboprop regional aircraft wing MDPI ", *Biomimetics*, Vol. 4 No. 3, pp. 1-20.

Linkoping, SweedenNelson, R.C. (2007), *Flight Stability and Automatic Control*, 2nd ed. McGraw-Hill, New York, NY.

Oktay, T. and Sultan, C. (2013), "Simultaneous helicopter and control system design", *Journal of Aircraft*, Vol. 50 No. 3, pp. 206-222.

Oktay, T., Konar, M., Onay, M., Aydin, M. and Abdallah Mohamed, M. (2016), "Simultaneous small UAV and autopilot system design", *Aircraft Engineering and Aerospace Technology*, Vol. 88 No. 6.

Raymer, D.P. (1992), "Aircraft design: a conceptual approach", AIAA Education Series, pp. 58-59.

Sadegh, P. and Spall, J.C. (1998), "Optimal random perturbations for multivariable stochastic approximation using a simultaneous perturbation gradient approximation", *IEEE Transactions on Automatic Control*, Vol. 43 No. 10, pp. 1480-1484.

Sahin, H., Kose, O. and Oktay, T. (2022), "Simultaneous autonomous system and powerplant design for morphing quadrotors", *Aircraft Engineering and Aerospace Technology*, Vol. 94 No. 8, pp. 1228-1241.

Sal, F. (2023), "Simultaneous swept anhedral helicopter blade tip shape and control-system design", *Aircraft Engineering and Aerospace Technology*, Vol. 95 No. 1, doi: 10.1108/AEAT-02-2022-0050.

Sedin, Y.C.H., Persson, I. and Sillen, M. (2004), "Computational analysis and re-design of a wing-strake combination", 24th International Congress Of The Aeronautical Sciences, Linkoping, Sweeden.

Silva, V.T., Lundbladh, A., Xisto, C. and Grönstedt, T. (2023), "Over-wing integration of ultra-high bypass ratio engines: a coupled wing redesign and engine position study", *Aerospace Science and Technology*, Vol. 138, pp. 1-18.

Uzun, M. and Oktay, T. (2023), "Simultaneous UAV having actively sweep angle morphing wing and flight control system design", *Aircraft Engineering and Aerospace Technology*, Vol. 95 No. 7, pp. 1062-1068.

Appendix

Table A1 Nomenclature

Symbol	Explanation
u, v, w	UAV linear velocity components (i.e. longitudinal lateral, vertical, respectively), [m/s]
p, q, r	UAV angular velocity components (i.e. longitudinal lateral, vertical, respectively), [deg/s]
ϕ_A, θ_A, ψ_A	UAV Euler angle components (i.e. longitudinal lateral, vertical, respectively), [deg]
$\delta_T, \delta_e, \delta_a, \delta_t$	Controls of throttle, elevator, aileron and rudder [deg]
h	Altitude of the UAV, [m]
J	Autonomous system cost, [ ]
V	Intensity of sensor noise, [ ]
W	Intensity of process noise, [ ]
Θ_{W_i}	Incidence angle of the UAV, [deg]
C_{D_0}, C_{L_0}, C_L	Reference drag coeff., Reference lift coeff., Aircraft lift coeff., [ ]
Λ	Wing sweep angle

Source: Table courtesy of Uzun

Table A2 Specific data of the ISTE-UAV

Physical property	Its magnitude
Total weight	2.185 kg
Wing span	1.3 m
Wing area	0.325 m^2
Aspect ratio of wing	5.2
Interval of the wing incidence angle	between 0° and 10°
Passively morphing wing incidence angle property	Yes
Taper ratio of the wing	Untapered
Sweep angle of the wing	Not applied for this research paper
Type of the powerplant	Battery-powered electrical system

Source: Table courtesy of Uzun

Table A3 Abbreviations

Physical property	Its explanation
AR	Aspect ratio
FCS	Flight control system
ISTE	Iskenderun Technical University
SPSA	Simultaneous perturbation stochastic approximation
UAV	Unmanned aerial vehicle

Source: Table courtesy of Uzun

Table A4 Terms in the state space model for the ISTE-UAV

Physical property	Its explanation
X_u	The contribution of the change in the velocity u to the change of X force
C_{X_u}	The stability derivative coefficient related with X_u
X_w	The contribution of the change in the velocity w to the change of X force
Z_u	The contribution of the change in the velocity u to the change of Z force
C_{Z_u}	The stability derivative coefficient related with Z_u
Z_w	The contribution of the change in the velocity w to the change of Z force
M_u	The contribution of the change in the velocity u to the change of M moment
$M\dot{w}$	The contribution of the change in the $\dot{w}$ to the change of M moment
M_q	The contribution of the change in the angular velocity q to the change of M moment
X_{δ_T}	The contribution of the change in the throttle to the change of X force
X_{δ_e}	The contribution of the change in the elevator to the change of X force
Z_{δ_T}	The contribution of the change in the throttle to the change of Z force
Z_{δ_e}	The contribution of the change in the elevator to the change of Z force
M_{δ_T}	The contribution of the change in the throttle to the change of M moment
M_{δ_e}	The contribution of the change in the elevator to the change of Z moment
Z_{δ_e}	The contribution of the change in the elevator to the change of Z force
Y_v	The contribution of the change in the velocity v to the change of Y moment
Y_p	The contribution of the change in the angular velocity p to the change of Y moment
C_{Y_p}	The stability derivative coefficient related with Y_p
Y_r	The contribution of the change in the angular velocity r to the change of Y moment
L^*_w	starred contribution of the change in the velocity w to the change of L moment
L^*_p	starred contribution of the change in the angular velocity p to the change of L moment
L^*_r	starred contribution of the change in the angular velocity r to the change of L moment
L^*_v	starred contribution of the change in the velocity v to the change of L moment
N^*_v	starred contribution of the change in the velocity v to the change of N moment
N^*_p	starred contribution of the change in the angular velocity P to the change of N moment
N^*_r	starred contribution of the change in the angular velocity r to the change of N moment
Y_{δ_r}	contribution of the change in the rudder to the change of Y force
$L^*_{\delta_a}$	starred contribution of the change in the aileron to the change of L moment
$L^*_{\delta_r}$	starred contribution of the change in the rudder to the change of L moment
$N^*_{\delta_a}$	starred contribution of the change in the aileron to the change of N moment
$N^*_{\delta_r}$	starred contribution of the change in the rudder to the change of N moment
I_x, I_z, i_{xz}	Inertial terms of the UAV

Note: The starred versions are obtained by dividing the stability derivative with [1-(Ixz^2/(Ix*Iz)]
Source: Table courtesy of Uzun

Corresponding author
Metin Uzun can be contacted at: metin.uzun@iste.edu.tr